PHYSICAL REVIEW B **83**, 140512(R) (2011)

Emergence of fully gapped s_{++}-wave and nodal d-wave states mediated by orbital and spin fluctuations in a ten-orbital model of KFe_2Se_2

Tetsuro Saito,[1] Seiichiro Onari,[2] and Hiroshi Kontani[1]

[1]*Department of Physics, Nagoya University and JST, TRIP, Furo-cho, Nagoya 464-8602, Japan*

[2]*Department of Applied Physics, Nagoya University and JST, TRIP, Furo-cho, Nagoya 464-8602, Japan*

(Received 28 February 2011; revised manuscript received 23 March 2011; published 22 April 2011)

We study the superconducting state in recently discovered high-T_c superconductor $K_xFe_2Se_2$ based on the ten-orbital Hubbard-Holstein model without hole pockets. When the Coulomb interaction is large, a spin-fluctuation-mediated d-wave state appears due to the nesting between electron pockets. Interestingly, the symmetry of the body-centered tetragonal structure in $K_xFe_2Se_2$ requires the existence of nodes in the d-wave gap, although a fully gapped d-wave state is realized in the case of a simple tetragonal structure. In the presence of moderate electron-phonon interaction due to Fe-ion optical modes, however, orbital fluctuations give rise to the fully gapped s_{++}-wave state without sign reversal. Therefore, both superconducting states are distinguishable by careful measurements of the gap structure or the impurity effect on T_c.

DOI: 10.1103/PhysRevB.83.140512 PACS number(s): 74.70.Xa, 74.20.Fg, 74.20.Rp

The pairing mechanism of high-T_c iron-based superconductors has been a significant open problem. The main characteristics of FeAs compounds are (i) the nesting between electron pockets (e-pockets) and hole pockets (h-pockets), and (ii) the existence of an orbital degree of freedom. By focusing on the intra-orbital nesting, a fully gapped, sign-reversing s-wave state ($s_{\pm}$-wave state) was predicted based on the spin-fluctuation theories.[1,2] However, the existence of moderate electron-phonon (e-ph) interactions due to Fe-ion optical phonons and the interorbital nesting can produce large orbital fluctuations.[3] Then, an orbital-fluctuation-mediated s-wave state without sign reversal (s_{++}-wave state) was predicted by using the random-phase-approximation (RPA)[3,4] or fluctuation-exchange (FLEX) approximation method.[5] According to the analysis in Refs. 6 and 7, the s_{++}-wave state is consistent with the robustness of T_c against randomness[8,9] as well as the "resonancelike" hump structure in the neutron inelastic scattering.[10] Non-Fermi liquid transport phenomena in ρ (Ref. 11) can be explained by the development of orbital fluctuations.[5]

Recently, iron-selenium 122-structure compound $A_xFe_2Se_2$ ($A=$ alkaline metals) with $T_c \sim 30$ K was discovered.[12] This heavily electron-doped superconductor has been attracting great attention since both the band calculations[13,14] and angle-resolved photoemission spectrum (ARPES) measurements[15–17] indicate the absence of h-pockets. NMR measurements report the weakness of spin fluctuations,[18] and both ARPES[15–17] and specific heat measurements[19] indicate the isotropic superconducting (SC) gap. Thus, the study of $A_xFe_2Se_2$ will give us important information to reveal the pairing mechanism of iron pnictides.

The unit cell of iron-based superconductors contains two Fe atoms. However, except for 122 systems, one can construct a simple "single-Fe model" from the original "two-Fe model" by applying the gauge transformation on d orbitals.[20] By this procedure, the original Brillouin zone (BZ) is enlarged to the "unfolded BZ." Based on the single-Fe model, a spin-fluctuation-mediated d-wave state (B_{1g} representation) "without nodes" was proposed[21–23] by focusing on the nesting between e-pockets. However, we cannot construct a single-Fe model for 122 systems, since finite hybridization between e-pockets prevents the unfolding procedure.[20] Therefore, a theoretical study based on the original two-Fe model is highly desired to conclusively define the gap structure.

In this Rapid Communication, we study the ten-orbital (two Fe atoms) Hubbard-Holstein (HH) model for KFe_2Se_2 using the RPA method. When the Coulomb interaction is large, we obtain the d-wave SC state due to the spin fluctuations, as predicted by the recent theoretical studies in the single-Fe Hubbard models.[21–23] However, the gap function on the Fermi surfaces (FSs) inevitably has a "nodal structure" in the two-Fe model, due to the symmetry requirement of the body-centered tetragonal lattice. However, an orbital-fluctuation-mediated s_{++}-wave state is realized by small e-ph coupling; the dimensionless coupling constant $\lambda = gN(0)$ is just ~ 0.2. Since the nodal SC state is fragile against randomness, study of the impurity effect will be useful to distinguish these SC states.

We perform the local-density-approximation (LDA) band calculation for KFe_2Se_2 using WIEN2K code based on the experimental crystal structure.[12] Next, we derive the ten-orbital tight-binding model that reproduces the LDA band structure and its orbital character using WANNIER90 code and WIEN2WANNIER interface.[24] The dispersion of the model and the primitive BZ are shown in Figs. 1(a) and 1(b). Based on a similar ten-orbital model, Suzuki *et al.* studied the $s_{\pm}$-wave gap structure for $BaFe_2As_2$.[25]

In Fig. 1, we show the FSs of KFe_2Se_2 for $k_z = 0$ [Fig. 1(c)] and $k_z = \pi$ [Fig. 1(d)] planes when the electron number per Fe ion is $n = 6.5$. On each plane, there are four large and heavy e-pockets around the X and Y points, and one small and light e-pocket around the Z point. For $n = 6.5$, the energy of the h band at Γ point from the Fermi level E_h is about -0.07 eV. Since the obtained FS topology and the value of E_h are consistent with recent reports using ARPES measurements,[15–17] we study the case $n = 6.5$ hereafter. In the present BZ in Fig. 1(b), Γ and Z points and X and Y points in Fig. 1(c) are not equivalent, and $k_z = 2\pi$ plane is given by shifting the points in Fig. 1(c) by (π,π). As for Fig. 1(d), T and T' points and P and P' points are equivalent, meaning that the reciprocal wave vector on

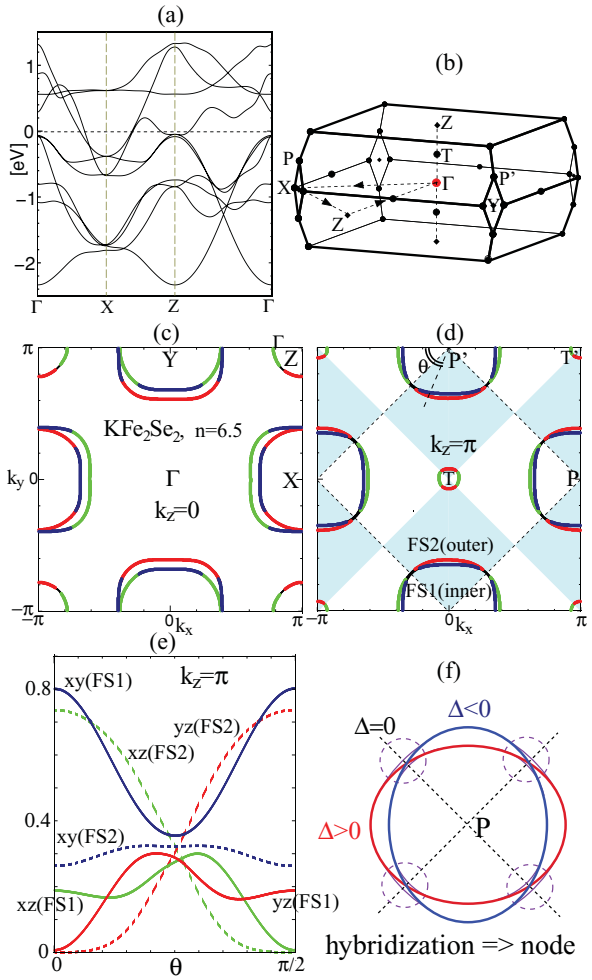

FIG. 1. (Color online) (a) Dispersion of the present ten-orbital model for KFe_2Se_2. Γ, X, and Z points are on the $k_z = 0$ plane. (b) Primitive BZ for body-centered tetragonal lattice. (c),(d) FSs on the $k_z = 0$ plane and $k_z = \pi$ plane. The green (light gray), red (gray), and blue (dark gray) lines correspond to xz, yz, and xy orbitals, respectively. The diamond-shaped shadows in (d) indicate the sign of the basis function for the B_{1g} representation. (e) Weight of each orbital on the inner FS (FS1) and the outer FS (FS2) as a function of θ; θ is shown in (d). (f) Hybridization between two e-pockets in 122 systems should create the nodal d-wave gap.

the $k_z = \pi$ plane is (π,π) and $(\pi, -\pi)$. The diamond-shaped shadows in the $k_z = \pi$ plane indicate the sign of basis function for B_{1g} [$(x^2 - y^2)$-type] representation, which has nodes on the P-P' line on both FS1 (inner FS) and FS2 (outer FS).

To confirm the existence of nodes, we verify that FS1 and FS2 in KFe_2Se_2 are largely hybridized. In fact, the weights of d orbitals on FS1 and FS2 given in Fig. 1(e) are smooth functions of θ, which is strong evidence for the hybridization in wide momentum space. This hybridization disappears when interlayer hoppings are neglected. Then, both xy (FS1) and xy (FS2) show cusps at $\theta = \pi/4$, and xz (FS2) suddenly drops to almost zero for $\theta \geqslant \pi/4$. In Fig. 1(f), we explain the origin of the nodal gap based on the fully gapped d-wave solution in the single-Fe model.[21–23] By introducing interlayer hoppings, two elliptical e-pockets with positive and negative Δ in the unfolded BZ are hybridized to form FS1 and FS2 with fourfold

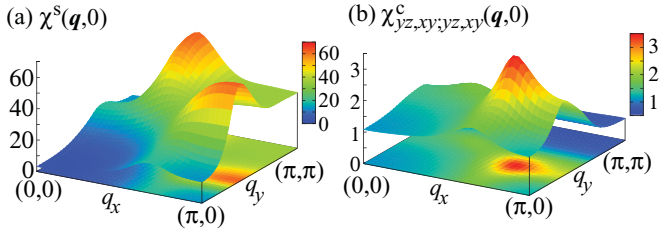

FIG. 2. (Color online) (a) $\chi^s(\boldsymbol{q},0)$ for $U = 1.1$ eV and $g = 0$, and (b) $\chi^c_{yz,xy;yz,xy}(\boldsymbol{q},0)$ for $U = 0$ and $g = 0.22$ eV.

symmetry. As a result, nodal lines inevitably emerge on FS1 and FS2, at least near the $|k_z| = \pi$ plane.

Here, we study the ten-orbital HH model using the RPA method. As for the Coulomb interaction, we consider the intraorbital term U, the interorbital term U', Hund's coupling or pair hopping J, and assume the relation $U = U' + 2J$ and $J = U/6$. In addition, we consider the e-ph interaction due to Fe-ion optical phonons; the phonon-mediated electron-electron interaction $(-g)$ and its matrix elements are presented in Ref. 4. Hereafter, we perform the RPA on the two-dimensional planes for $k_z = 0, \pi/2$, and π.

For $n = 6.5$ and $k_z = 0$, the critical value of g for the orbital-density wave (ODW) is $g_c = 0.23$ eV for $U = 0$, and the critical value of U for the spin-density wave (SDW) is $U = 1.18$ eV for $g = 0$. These values change only ∼2% for different k_z. The obtained U-g phase diagram is very similar to Fig. 2 in Ref. 4, irrespective of the absence of h-pockets in KFe_2Se_2. The reason would be that (i) the density of states (DOS) in KFe_2Se_2 is about 1 eV^{-1} per Fe, which is comparable with other iron pnictides, and (ii) the nesting between e-pockets is rather strong because of their squarelike shape. Figure 2(a) shows the total spin susceptibility $\chi^s(\boldsymbol{q},0)$ at $U = 1.1$ eV and $g = 0$ for the $k_z = 0$ plane. χ^s is given by the intra-orbital nesting, and its peak position is $\boldsymbol{q} \approx (\pi, 0.4\pi)$, which is consistent with previous studies.[21–23] The obtained incommensurate spin correlation is the origin of the d-wave SC gap. Figure 2(b) shows the off-diagonal orbital susceptibility $\chi^c_{yz,xy;yz,xy}(\boldsymbol{q},0)$ for the $k_z = 0$ plane at $U = 0$ and $g = 0.22$ eV; its definition is given in Refs. 3–5. It is derived from the inter-orbital nesting between xz and xy, and its peak position is $\boldsymbol{q} \approx (0.7\pi, 0.4\pi)$. Note that the peak position of $\chi^c_{xz,xy;xz,xy}$ is $\boldsymbol{q} \approx (0.4\pi, 0.7\pi)$. The obtained strong spin and orbital correlations are the origin of the d-wave and s_{++}-wave SC states.

In the following, we solve the linearized gap equation to obtain the gap function by applying the Lanczos algorithm to achieve reliable results. In the actual calculation results shown below, we take 64×64 $\boldsymbol{k}$-point meshes and 512 Matsubara frequencies. First, we study the spin-fluctuation-mediated SC state for $U \lesssim U_c$ by putting $g = 0$. Figures 3(a)–3(c) show the gap functions of the d-wave solution at $T = 0.03$ eV for $k_z = 0, \pi/2$, and π, respectively. In the case of $U = 1.1$ eV, the eigenvalue λ_E is 0.61 for Fig. 3(a), 0.63 for Fig. 3(b), and 0.62 for Fig. 3(c); the relation $\lambda_E \geqslant 1$ corresponds to the SC state. They are relatively small since the SC condensation energy becomes small when the SC gap has a complicated nodal-line structure. On the $k_z = \pi$ plane in Fig. 3(c), the nodal lines are along $\theta = \pi/4$ and $3\pi/4$ directions, which is consistent

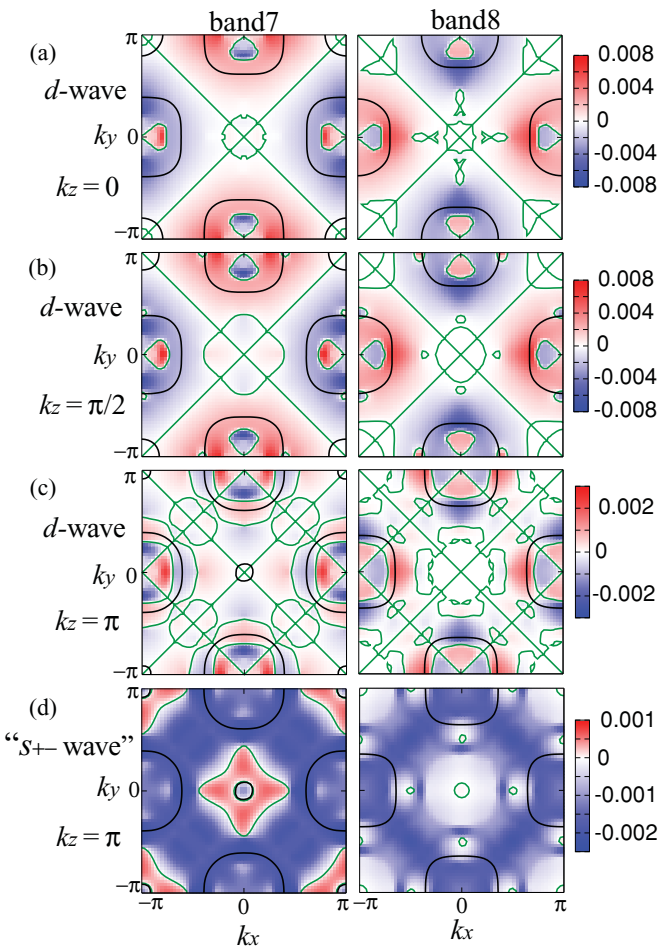

FIG. 3. (Color online) SC gap functions for outer FS (FS2) on band 7 and inner FS (FS1) on band 8: d-wave gap functions on the (a) $k_z = 0$, (b) $k_z = \pi/2$, and (c) $k_z = \pi$ planes. Black and green (gray) lines represent the FSs and gap nodes. (d) $s_{\pm}$-wave gap function on the $k_z = \pi$ plane.

with the basis of the B_{1g} representation in Fig. 1(d). These nodes move to near the BZ boundary, $\theta = 0$ and π, on the $k_z = \pi/2$ plane in Fig. 3(b), and they deviate from the FSs on the $k_z = 0$ plane in Fig. 3(a). As a result, the nodal gap appears for $\pi/2 < |k_z| < 3\pi/2$ in the whole BZ, $|k_z| \leqslant 2\pi$.

We also obtain the $s_{\pm}$-wave state, with the sign reversal of the SC gap between e-pockets and the "hidden h-pockets below the Fermi level" given by the valence bands 5 and 6. The obtained solution is shown in Fig. 3(d) for $k_z = \pi$. Interestingly, the obtained eigenvalue is $\lambda_E = 0.99$ for $U = 1.1$ eV, which is larger than λ_E for the d-wave state in Figs. 3(a)–3(c). Such large λ_E originates from the scattering of Cooper pairs between e-pockets and the hidden h-pockets, which was discussed as the "valence-band Suhl-Kondo (VBSK) effect" in the study of Na_xCoO_2 in Ref. 26.

Here, we analyze the T dependence of λ_E based on a simple two-band model with interband repulsion. The set of gap equations is given by[26] $\lambda_E \Delta_h = -V N_e L_e \Delta_e$ and $\lambda_E \Delta_e = -V N_h L_h \Delta_h$, where $V > 0$ is the repulsive interaction between e- and h-pockets, and $N_{e,h}$ is the DOS near the Fermi level. When the top of the h-pocket is well above the Fermi level (case 1), $L_e = L_h = \ln(1.13\omega_c/T)$,

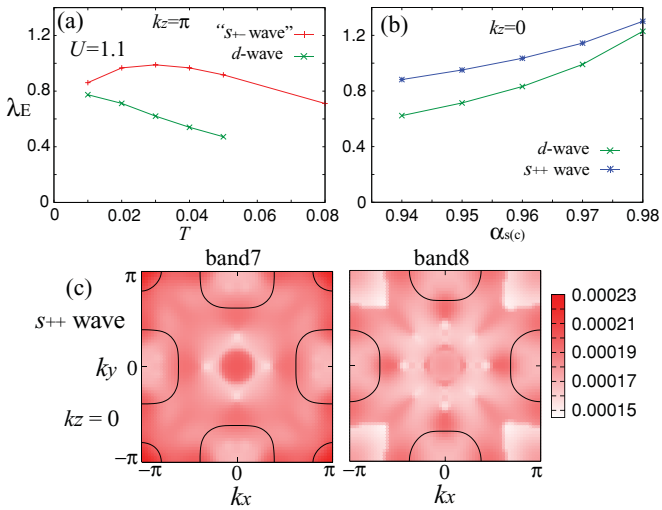

FIG. 4. (Color online) (a) T dependence of λ_E for d- and $s_{\pm}$-wave states. λ_E at $T = 0.01$ eV is underestimated because of the shortage of $\boldsymbol{k}$- and Matsubara-meshes. (b) α_s (α_c) dependence of λ_E for d-wave (s_{++}-wave) state at $T = 0.03$ eV. (c) SC gap functions for the s_{++}-wave state.

where ω_c is the cutoff energy. Thus, the eigenvalue is given as $\lambda_E = V\sqrt{N_e N_h}\ln(1.13\omega_c/T) \propto -\ln T$, which is similar to single-band BCS superconductors. However, when h-pocket is slightly below the Fermi level (case 2), $L_h = (1/2)\ln(\omega_c/|E_h|)$, where $E_h < 0$ is the energy of the top of the h-band.[26] Thus, the eigenvalue is given as $\lambda_E = V\sqrt{N_e N_h L_h}\sqrt{\ln(1.13\omega_c/T)} \propto \sqrt{-\ln T}$. Therefore, in case 2, the T dependence of λ_E is much more moderate. In fact, as shown in Fig. 4(a), λ_E for the d-wave state increases monotonically with decreasing T, while λ_E for the $s_{\pm}$-wave state saturates at low temperatures. This result suggests that the d-wave state overcomes the $s_{\pm}$-wave state at $T_c \sim 30$ K in $K_xFe_2Se_2$. Although T_c in the $s_{\pm}$-wave state is ~ 0.06 eV in Fig. 4(a), it is greatly reduced by the self-energy correction that is absent in the RPA.[5]

We now discuss the VBSK effect for the $s_{\pm}$-wave state in more detail. According to the inelastic neutron-scattering measurement of $Ba(Fe,Co)_2As_2$,[10] the characteristic spin-fluctuation energy is $\omega_{sf} \sim 100$ K, just above $T_c \sim 30$ K. If we assume a similar ω_{sf} in KFe_2Se_2, since T_c is close, we obtain the relation $\omega_c \sim \omega_{sf} \ll |E_h|$ in KFe_2Se_2. Since L_h is a monotonic decrease function of $|E_h|/\omega_c$ and $L_h < 1$ for $-E_h/\omega_c > 0.15$, we consider that the d-wave state overcomes the $s_{\pm}$-wave state in KFe_2Se_2, as far as the spin-fluctuation-mediated superconductivity is concerned. Although a high-T_c $s_{\pm}$-wave state might be realized for $|E_h|/\omega_c < 0.1$, the realized T_c will be very sensitive to E_h or the filling n.[26]

Now, we study the s_{++}-wave state due to orbital fluctuations on the $k_z = 0$ plane with $n = 6.5$. In Fig. 4(b), we show the α_c dependence of λ_E at $T = 0.03$ for the s_{++}-wave state with $U = 0$, and the α_s dependence of λ_E for the d-wave state with $g = 0$. Here, α_c (α_s) is the charge (spin) Stoner factor introduced in Ref. 3; $\alpha_c = 1$ ($\alpha_s = 1$) corresponds to the ODW (SDW) state. In calculating the s_{++}-wave state, we use much larger phonon energy, $\omega_D = 0.15$ eV, considering that the calculating temperature is about ten times larger than the

real T_c. The SC gap functions for the s_{++}-wave state are rather isotropic, as shown in Fig. 4(c). However, the obtained SC gap becomes more anisotropic in the case of $U > 0$.[5]

We stress that the RPA is insufficient for the quantitative study of λ_E since the self-energy correction Σ is dropped. In Ref. 5, we have studied the present model based on their FLEX approximation, and found that the critical region with $\alpha_c \gtrsim 0.95$ is enlarged by the inelastic scattering $\gamma = \mathrm{Im}\Sigma$. Also, the γ-induced suppression in λ_E for d- or $s_{\pm}$-wave states is more prominent than that for the s_{++}-wave state, since γ due to spin fluctuations is larger than that due to orbital fluctuations.[5]

Recently, we found the paper by Mazin,[27] in which the k_z dependence of the nodal d-wave gap in Fig. 4 corresponds to Figs. 3(a)–3(c) in the present work.

In summary, we studied the mechanism of superconductivity in KFe_2Se_2 based on the ten-orbital HH model without h-pockets. Similar to iron-pnictide superconductors, an orbital-fluctuation-mediated s_{++}-wave state is realized by small dimensionless e-ph coupling constant $\lambda = gN(0) \sim 0.2$. We also studied the spin-fluctuation-mediated d-wave state, and confirmed that nodal lines appear on the large e-pockets due to the hybridization between two e-pockets that is inherent in 122 systems. Therefore, careful measurements on the SC gap anisotropy are useful to distinguish these different pairing mechanisms. The study of the impurity effect on T_c is also useful since the d-wave (and $s_{\pm}$-wave) state is fragile against impurities.

We are grateful to D. J. Scalapino, P. Hirschfeld, A. Chubukov, and Y. Matsuda for useful and stimulating discussions at the KITP 2011 international workshop, Iron-Based Superconductors. This study has been supported by Grants-in-Aid for Scientific Research from MEXT of Japan, and by JST, TRIP. Numerical calculations were performed using the facilities of the supercomputer centers in ISSP and Institute for Molecular Science.

[1] I. I. Mazin, D. J. Singh, M. D. Johannes, and M. H. Du, Phys. Rev. Lett. **101**, 057003 (2008).
[2] K. Kuroki, S. Onari, R. Arita, H. Usui, Y. Tanaka, H. Kontani, and H. Aoki, Phys. Rev. Lett. **101**, 087004 (2008).
[3] H. Kontani and S. Onari, Phys. Rev. Lett. **104**, 157001 (2010).
[4] T. Saito, S. Onari, and H. Kontani, Phys. Rev. B **82**, 144510 (2010).
[5] S. Onari and H. Kontani, e-print arXiv:1009.3882 (to be published).
[6] S. Onari and H. Kontani, Phys. Rev. Lett. **103**, 177001 (2009).
[7] S. Onari, H. Kontani, and M. Sato, Phys. Rev. B **81**, 060504(R) (2010).
[8] A. Kawabata, S. C. Lee, T. Moyoshi, Y. Kobayashi, and M. Sato, J. Phys. Soc. Jpn. **77**, 103704 (2008); M. Sato, Y. Kobayashi, S. C. Lee, H. Takahashi, E. Satomi, and Y. Miura, *ibid.* **79**, 014710 (2010); S. C. Lee, E. Satomi, Y. Kobayashi, and M. Sato, *ibid.* **79**, 023702 (2010).
[9] Y. Nakajima, T. Taen, Y. Tsuchiya, T. Tamegai, H. Kitamura, and T. Murakami, e-print arXiv:1009.2848 (to be published).
[10] A. D. Christianson, E. A. Goremychkin, R. Osborn, S. Rosenkranz, M. D. Lumsden, C. D. Malliakas, I. S. Todorov, H. Claus, D. Y. Chung, M. G. Kanatzidis, R. I. Bewley, and T. Guidi, Nature (London) **456**, 930 (2008); Y. Qiu, W. Bao, Y. Zhao, C. Broholm, V. Stanev, Z. Tesanovic, Y. C. Gasparovic, S. Chang, J. Hu, B. Qian, M. Fang, and Z. Mao, Phys. Rev. Lett. **103**, 067008 (2009); D. S. Inosov, J. T. Park, P. Bourges, D. L. Sun, Y. Sidis, A. Schneidewind, K. Hradil, D. Haug, C. T. Lin, B. Keimer, and V. Hinkov, Nature Phys. **6**, 178 (2010).
[11] S. Kasahara, T. Shibauchi, K. Hashimoto, K. Ikada, S. Tonegawa, R. Okazaki, H. Shishido, H. Ikeda, H. Takeya, K. Hirata, T. Terashima, and Y. Matsuda, Phys. Rev. B **81**, 184519 (2010).
[12] J. Guo, S. Jin, G. Wang, S. Wang, K. Zhu, T. Zhou, M. He, and X. Chen, Phys. Rev. B **82**, 180520(R) (2010).
[13] I. R. Shein and A. L. Ivanovskii, e-print arXiv:1012.5164 (to be published).
[14] I. A. Nekrasov and M. V. Sadovskii, Pis'ma Zh. Eksp. Teor. Fiz. [JETP Lett.] **93**, 182 (2011).
[15] Y. Zhang, L. X. Yang, M. Xu, Z. R. Ye, F. Chen, C. He, H. C. Xu, J. Jiang, B. P. Xie, J. J. Ying, X. F. Wang, X. H. Chen, J. P. Hu, M. Matsunami, S. Kimura, and D. L. Feng, Nature Mater. **10**, 273 (2011).
[16] T. Qian, X.-P. Wang, W.-C. Jin, P. Zhang, P. Richard, G. Xu, X. Dai, Z. Fang, J.-G. Guo, X.-L. Chen, and H. Ding, e-print arXiv:1012.6017 (to be published).
[17] L. Zhao, D. Mou, S. Liu, X. Jia, J. He, Y. Peng, L. Yu, X. Liu, G. Liu, S. He, X. Dong, J. Zhang, J. B. He, D. M. Wang, G. F. Chen, J. G. Guo, X. L. Chen, X. Wang, Q. Peng, Z. Wang, S. Zhang, F. Yang, Z. Xu, C. Chen, and X. J. Zhou, e-print arXiv:1102.1057 (to be published).
[18] W. Yu, L. Ma, J. B. He, D. M. Wang, T.-L. Xia, and G. F. Chen, e-print arXiv:1101.1017 (to be published).
[19] B. Zeng, B. Shen, G. Chen, J. He, D. Wang, C. Li, and H.-H. Wen, e-print arXiv:1101.5117 (to be published).
[20] T. Miyake, K. Nakamura, R. Arita, and M. Imada, J. Phys. Soc. Jpn. **79**, 044705 (2010).
[21] F. Wang, F. Yang, M. Gao, Z.-Y. Lu, T. Xiang, and D.-H. Lee, Europhys Lett. **93**, 57003 (2011).
[22] T. A. Maier, S. Graser, P. J. Hirschfeld, and D. J. Scalapino, e-print arXiv:1101.4988 (to be published).
[23] T. Das and A. V. Balatsky, e-print arXiv:1101.6056 (to be published).
[24] J. Kunes, R. Arita, P. Wissgott, A. Toschi, H. Ikeda, and K. Held, Comput. Phys. Commun. **181**, 1888 (2010).
[25] K. Suzuki, H. Usui, and K. Kuroki, J. Phys. Soc. Jpn. **80** 013710 (2011).
[26] K. Yada and H. Kontani, Phys. Rev. B **77**, 184521 (2008); J. Phys. Soc. Jpn. **75**, 033705 (2006).
[27] I. I. Mazin, e-print arXiv:1102.3655 (to be published).